JOURNAL OF CHEMICAL EDUCATION

Laboratory Experiment

pubs.acs.org/jchemeduc

Equilibrium between Different Coordination Geometries in Oxidovanadium(IV) Complexes

Valeria Ugone,[†] Eugenio Garribba,[†] Giovanni Micera,[†] and Daniele Sanna*[,‡]

[†]Dipartimento di Chimica e Farmacia, Università di Sassari, Via Vienna 2, I-07100 Sassari, Italy

[‡]Istituto C.N.R. di Chimica Biomolecolare, Trav. La Crucca 3, I-07040 Sassari, Italy

Supporting Information

ABSTRACT: In this laboratory activity, the equilibrium between square pyramidal and octahedral $V(IV)O^{2+}$ complexes is described. We propose a set of experiments to synthesize and characterize two types of $V(IV)O^{2+}$ complexes. The experiment allows great flexibility and may be effectively used at a variety of levels and the activity can be lengthened or shortened depending on the available time. The laboratory practice can combine various experiments: (i) synthesis of solid transition metal complexes, (ii) analysis of the solid complexes to hypothesize their coordination geometry, (iii) measurement of room temperature and frozen solution EPR (Electron Paramagnetic Resonance) spectra obtained when dissolving the solid complexes in different solvents, (iv) software simulation of room temperature and frozen solution EPR spectra, (v) measurement of UV−vis spectra of solutions obtained when dissolving the solid complexes in different solvents, (vi) optimization of the coordination geometry of $V(IV)O^{2+}$ complexes with DFT calculations, (vii) calculation of the EPR parameters of $V(IV)O^{2+}$ complexes with DFT methods, and (viii) influence of the temperature on the equilibrium calculated using DFT methods. The activity is organized to guide the students towards to a plausible explanation of the experimental evidence.

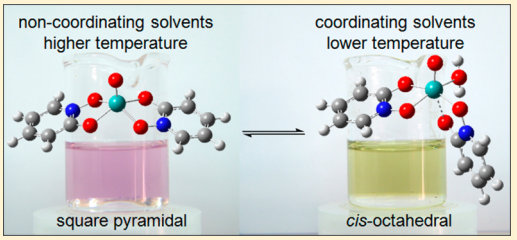

KEYWORDS: *Upper-Division Undergraduate, Inorganic Chemistry, Problem Solving/Decision Making, Aqueous Solution Chemistry, Computational Chemistry, Coordination Compounds, EPR/ESR Spectroscopy, Equilibrium*

Because of the color changes, from blue to pink, the equilibrium between tetrahedral and octahedral cobalt(II) complexes is an excellent demonstration to illustrate Le Chatelier's principle.[1] The laboratory activity described here represents a valid alternative to illustrate the equilibrium between different coordination geometries in transition metal complexes. The activity is based on the results previously published by us.[2]

EXPERIMENT

To provide a suitable framework for students, vanadium chemistry, EPR technique and DFT methods may be discussed in two or three prelab lectures. The complete set of experiments needs three 3-h laboratory sessions: synthesis of the complexes in the first session, recording and interpreting the EPR spectra in the second session, followed by building input files for DFT calculations and extracting information from the output ones. A detailed description of the experiment is reported in the Students' Instructions in the Supporting Information.

Chemicals and Hazards

The two ligands are available from Sigma-Aldrich: pyridine-2-ol-1-oxide, 56413, and pyridine-2-thiol-1-oxide, 188549. The complexes were prepared from vanadium(IV) oxide sulfate hydrate, 204862, a Sigma-Aldrich product. The hazard statements of the chemicals can be found in the Supporting Information.

Synthesis of the Solid Compounds, Elemental Analysis, and Possible Coordination Geometry

The ligands, pyridine-2-ol-1-oxide (2-hydroxypyridine-*N*-oxide, hpo) and pyridine-2-thiol-1-oxide (2-mercaptopyridine-*N*-oxide, mpo), are shown in Scheme 1.

Scheme 1. Ligands

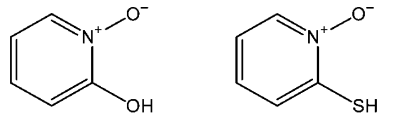

The solid compounds $[VO(hpo)_2]$ and $[VO(mpo)_2]$ can be synthesized according to the procedure described in the Students' Instructions and should be analyzed to obtain their elemental composition. The syntheses are relatively easy; the results of elemental analyses reported in the Supporting Information can be used to propose plausible coordination geometries of these complexes. Since the ligand molecules are

DOI: 10.1021/ed500794m
J. Chem. Educ. XXXX, XXX, XXX−XXX

bidentate, and assuming that V(IV) retains the oxido ligand,[3] the conclusion that the two complexes are pentacoordinated with two ligand molecules coordinated to vanadium should be reached. The presence of V═O group could be confirmed by IR spectroscopy; the stretching band of the V═O bond falls at 960 cm^{-1} for $[VO(mpo)_2]$ and at 984 cm^{-1} for $[VO(hpo)_2]$.[4] The X-ray structure reported for $[VO(mpo)_2]$[5,6] can be used to verify that the geometry of solid complexes is square pyramidal. There is no crystal structure for the complex $[VO(hpo)_2]$ but the same conclusion can be reached.

Behavior at Room Temperature in Coordinating and Non-coordinating Solvents

The solid compounds should be dissolved in coordinating (DMSO, DMF) and non-coordinating solvents (CH_2Cl_2, $CHCl_3$, toluene) and the room temperature EPR spectra recorded. The background of EPR spectroscopy has been discussed in this journal,[7] and some applications to the study of transition metal complexes and organic radicals were presented.[8,9] Some details are also given in the Supporting Information. The spectroscopic parameters (g and A values) of the experimental spectra should be measured and the results obtained in different solvents compared. To extract the parameters from the spectra, these latter can be simulated using the software Bruker WinEPR SimFonia[10] or EasySpin.[11]

At the beginning, the students can observe differences in the color of the solutions; for example dissolving the solid complex $[VO(hpo)_2]$ in CH_2Cl_2 the resulting solution is pink, while the same complex dissolved in DMSO gives a light green color (Supporting Information Figure S1). Since CH_2Cl_2 is a non coordinating solvent one could suppose that the square pyramidal coordination of the solid complex is retained. It could be also supposed that the light green color corresponds to another geometry which should involve also the solvent in the coordination.

An equilibrium between square pyramidal and octahedral geometry (with the additional coordination of a solvent molecule) is possible.[12] However, it is not easy to decide the ligand arrangement in the octahedral complexes. In fact both *trans-* (with water molecule *trans* to the oxido group) and *cis-*octahedral species (with water molecule *cis* to the oxido group) could be formed (Scheme 2). To decide which of these two

Scheme 2. Equilibra in $V(IV)O^{2+}$ Complexes

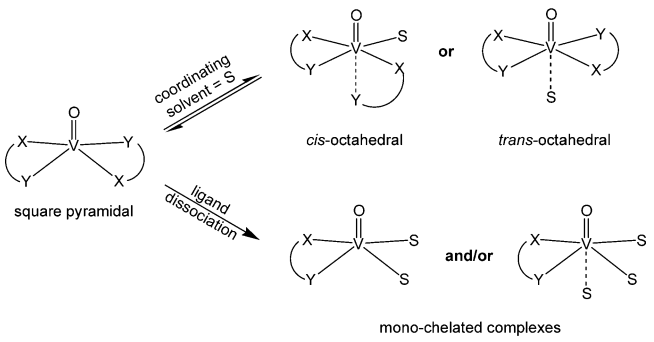

octahedral complexes is preferentially formed one should know that the hyperfine coupling constants, A_z and A_{iso}, are dependent by the donors coordinated in the equatorial plane and that the stronger the donors the lower the A_z and A_{iso} values. The experimental EPR spectra of $[VO(hpo)_2]$ in CH_2Cl_2 and in DMSO are reported in Figure 1 (traces a and b)

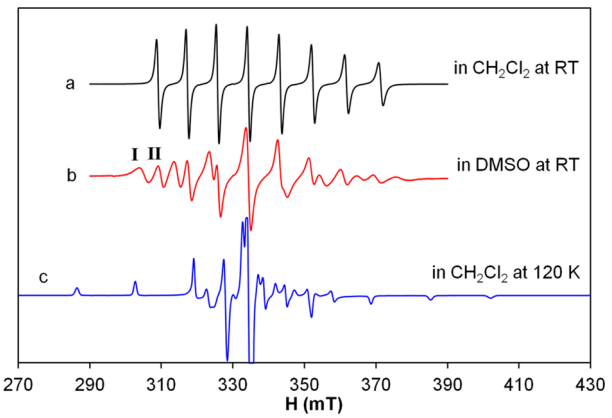

Figure 1. X-band EPR spectra recorded on solutions obtained dissolving $[VO(hpo)_2]$ in different solvents and temperatures. Spectrum (a) belongs to square pyramidal species $[VO(hpo)_2]$ with $A_{iso} = -82.1 \times 10^{-4}$ cm^{-1} and $g_{iso} = 1.977$ and the solution is pink. Spectrum (b) contains the resonances of **I**, *cis*-$[VO(hpo)_2(DMSO)]$ ($A_{iso} = -94.4 \times 10^{-4}$ cm^{-1}, $g_{iso} = 1.968$) and **II**, $[VO(hpo)_2]$ ($A_{iso} = -79.6 \times 10^{-4}$ cm^{-1}, $g_{iso} = 1.974$); the solution is green despite two species that are present. Spectrum (c) belongs to $[VO(hpo)_2]$ ($A_x = -41.0$, $A_y = -51.0$, $A_z = -150.6 \times 10^{-4}$ cm^{-1} and $g_x = 1.991$, $g_y = 1.981$, $g_z = 1.953$) and the solution is pink. All spectra reproduced or adapted with permission from ref 2. Copyright 2012 The Royal Society of Chemistry.

together with the measured parameters. Observing the different EPR spectra obtained, it is evident that the coordination geometry is dependent on the solvent. It is important to observe that in principle a solution with a certain color can contain more than one species. This fact can also be clearly observed, for example, in the EPR spectrum of the light green solution of $[VO(hpo)_2]$ in DMSO (Figure 1, trace b) where the signals of two species are present. From the spectra in Figure 1 (traces a and b) it is possible to observe that the only species present in CH_2Cl_2 is also present in DMSO (with the lower A_{iso} value), therefore the other species (with the higher A_{iso} value) could be the octahedral complex which confers the green color to the solution.

However, now it is only important to observe the solvent influence in the color of the solutions accompanying the changes in the EPR parameters. In the following paragraphs all the species formed in solution will be identified.

UV–Vis Spectra in Coordinating and Non-coordinating Solvents

UV–vis spectroscopy can be used to confirm the formation of different species. Dissolving the solid complex $[VO(hpo)_2]$ in CH_2Cl_2, it is possible to measure the spectrum (in the range 300–1000 nm) of the square pyramidal species, while it is impossible to experimentally measure the spectrum of the light green octahedral complex, because when dissolving the solid complex $[VO(hpo)_2]$ in DMSO a significant amount of the square pyramidal complex is also present. The spectrum of the octahedral isomer can be obtained by difference (Supporting Information Figure S7).

Behavior at Low Temperature in Coordinating and Non-coordinating Solvents and Comparison with the Results Obtained at Room Temperature

The results obtained at room temperature (RT) should be compared with those obtained with frozen solutions,[13] in order to establish if decreasing the temperature the structures are

DOI: 10.1021/ed500794m
J. Chem. Educ. XXXX, XXX, XXX–XXX

maintained or not. The conclusions should be in agreement with the color changes observed when freezing the solutions prepared at RT. Dissolving the solid complex $[VO(hpo)_2]$ in CH_2Cl_2 and DMSO the solutions have the same color (pink for CH_2Cl_2 and light green for DMSO) at room temperature and when are frozen, while dissolving the complex in DMF a color change from pink (at RT) to light green (at LT) should be observed, indicating a variation in the coordination geometry (Supporting Information Figure S2).

Some representative examples of room temperature and frozen solution spectra can be found in Figure 1 and in the Supporting Information. The frozen solution spectra can be simulated with the software Bruker WinEPR SimFonia,[10] or EasySpin[11] to obtain the values of A_i and g_i ($i = x, y, z$). The spin−orbit interaction between the ground and the excited states causes, in transition metal complexes, g to deviate from g_e; in the Supporting Information this is described in detail. To compare the parameters of room temperature and frozen solution EPR spectra, the relationship $A_{iso} = (A_x + A_y + A_z)/3$ should be used; in this way it is possible to decide if the coordination geometry is retained or not. If the experimental value of A_{iso}, measured at RT, is similar to that obtained from the frozen solution spectrum as $(A_x + A_y + A_z)/3$, A_{iso}^{expct}, the geometry is maintained, while if A_{iso} and A_{iso}^{expct} are different, the geometry changed.

For example, the complex $[VO(hpo)_2]$ dissolved in CH_2Cl_2 forms one species at 120 K (Figure 1, trace c) and the value of A_{iso}^{expct} is $(A_x + A_y + A_z)/3 = (-41.0 \times 10^{-4}\ cm^{-1} - 51.0 \times 10^{-4}\ cm^{-1} - 150.6 \times 10^{-4}\ cm^{-1})/3 = -80.9 \times 10^{-4}\ cm^{-1}$. Since this value is similar to that measured at RT (Figure 1, trace a, $A_{iso} = -82.1 \times 10^{-4}\ cm^{-1}$), it can be concluded that the geometry is retained.

On the other hand, for $[VO(hpo)_2]$ in DMSO, since two species are detected at RT (Figure 1, trace b, $A_{iso} = -79.6$ and $-94.4 \times 10^{-4}\ cm^{-1}$) but only one at 120 K (Supporting Information Figure S8), the value of A_{iso}^{expct} can help to determinate which species is present at low temperature. In fact, comparing the value of $A_{iso}^{expct} = -95.3 \times 10^{-4}\ cm^{-1}$ (obtained using the parameters $A_x = -57.5 \times 10^{-4}\ cm^{-1}$, $A_y = -60.5 \times 10^{-4}\ cm^{-1}$ and $A_z = -168.0 \times 10^{-4}\ cm^{-1}$) one can conclude that at 120 K only the isomer with the largest A_{iso} value is present.

The behavior of two complexes, $[VO(hpo)_2]$ and $[VO(mpo)_2]$, in different solvents and at different temperatures, RT and LT, is summarized in Table 1 and Supporting Information.

DFT Calculations: Optimization of the Structures and Calculation of EPR Parameters

DFT methods, applied to transition metal complexes, have been presented in some experiments in this journal.[14] The use of computational calculations can help to establish which of the possible species (square pyramidal, *cis*- or *trans*-octahedral) actually forms in solution.

In particular, density functional theory (DFT) calculations, incorporated in Gaussian 03,[15] can be used to optimize the geometry of $V(IV)O^{2+}$ complexes[16] and to calculate the EPR parameters.[17]

Depending on the relative arrangement of the ligands, two different isomers are possible both for square pyramidal, $[VO(hpo)_2]$ and $[VO(mpo)_2]$, (Scheme 3 and S1) and *trans*-octahedral complexes, *trans*-$[VO(hpo)_2(H_2O)]$ and *trans*-$[VO(mpo)_2(H_2O)]$ (Scheme 4 and S2). Concerning the hexa-coordinated complexes with *cis*-octahedral geometry, *cis*-$[VO(hpo)_2(H_2O)]$ and *cis*-$[VO(mpo)_2(H_2O)]$, four isomers are possible (Scheme 5 and Supporting Information Scheme S3). All the species are denoted with the IUPAC nomenclature[18] (see Supporting Information).

Table 1. Color of the Solutions Obtained Dissolving the Complex $[VO(hpo)_2]$ in Different Solvents

Solvent	Temperature[a]	Color	Species present in solution
CH_2Cl_2	RT	Pink	$[VO(hpo)_2]$[b]
	LT	Pink	$[VO(hpo)_2]$[b]
			cis-$[VO(hpo)_2(S)]$
$CHCl_3$/toluene	RT	Pink	$[VO(hpo)_2]$[b]
	LT	Pink	$[VO(hpo)_2]$[b]
			cis-$[VO(hpo)_2(S)]$
DMSO	RT	Green	$[VO(hpo)_2]$[b]
			cis-$[VO(hpo)_2(S)]$[b]
	LT	Green	*cis*-$[VO(hpo)_2(S)]$[b]
DMF	RT	Pink	$[VO(hpo)_2]$[b]
			cis-$[VO(hpo)_2(S)]$
	LT	Green	*cis*-$[VO(hpo)_2(S)]$[b]
			$[VO(hpo)_2]$

[a]RT indicates room temperature, LT is used for 77 and/or 120 K. [b]Predominant species.

Scheme 3. Possible Isomers for the Penta-Coordinated Species $[VO(hpo)_2]$

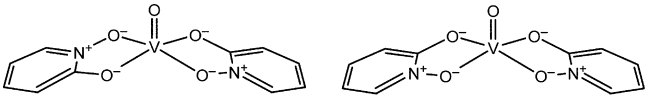

a) *SPY*-5-12 b) *SPY*-5-13

Scheme 4. Possible Isomers for the Complex *trans*-$[VO(hpo)_2(H_2O)]$

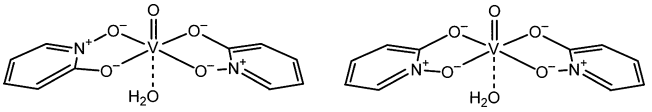

a) *OC*-6-42 b) *OC*-6-43

Scheme 5. Possible Isomers for the Complex *cis*-$[VO(hpo)_2(H_2O)]$

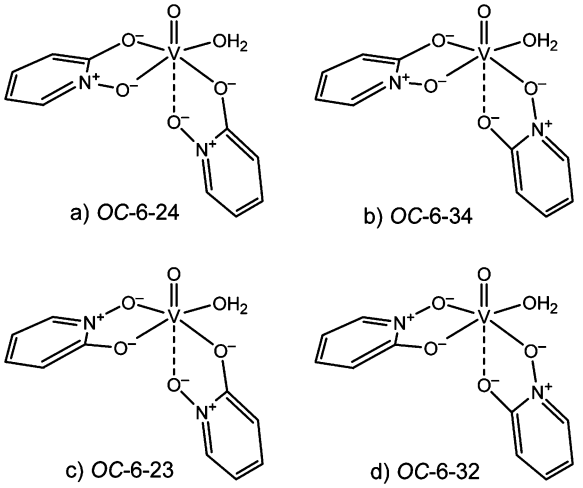

a) *OC*-6-24 b) *OC*-6-34 c) *OC*-6-23 d) *OC*-6-32

DOI: 10.1021/ed500794m
J. Chem. Educ. XXXX, XXX, XXX−XXX

Table 2. EPR Parameters of $V(IV)O^{2+}$ Species Formed by Hpo, Calculated at the Level of Theory BHandHLYP/6-311+g(d) with Gaussian[a]

Complex[b]	A_{iso}^{calcd}	A_{iso}	$\%\lvert A_{iso}\rvert$[c]	A_x^{calcd}	A_y^{calcd}	A_z^{calcd}	A_z	$\%\lvert A_z\rvert$[c]
SPY-5−12	−81.7	−82.1[d]	−0.5	−42.6	−52.5	−149.9	−150.6[d]	−0.5
SPY-5−13	−79.9		−2.7	−40.8	−51.0	−147.9		−1.8
OC-6−23	−96.0	−94.4[e]	1.7	−59.3	−63.2	−165.5	−168.0[e]	−1.5
OC-6−24	−95.6		1.3	−59.1	−62.8	−165.1		−1.7
OC-6−32	−94.2		−0.2	−57.9	−60.9	−163.8		−2.5
OC-6−34	−94.4		0.0	−58.8	−60.4	−164.0		−2.4
OC-6−42	−75.1		−20.5	−35.6	−47.0	−142.6		−15.1
OC-6−43	−74.4		−21.2	−34.9	−46.4	−141.9		−15.6

[a]All the values are in 10^{-4} cm^{-1}. [b]Nomenclature based on IUPAC recommendations, see ref 18. [c]Percentage deviation with respect to the absolute experimental value calculated as $100 \times (\lvert A_i\rvert^{calcd} - \lvert A_i\rvert)/\lvert A_i\rvert$, with i = *iso*, *z*. [d]Measured in CH_2Cl_2. [e]Measured in DMSO.

The values of A_{iso}, A_x, A_y and A_z calculated with Gaussian for the various possible complexes of hpo and mpo are reported in Tables 2 and Supporting Information Table S3.

Comparing the calculated (A_i^{calcd}) and the experimental (A_i) values it is possible to decide which species are present in solution. For example, comparing the data obtained by DFT calculations with the experimental values of A_{iso} and A_z for the complex $[VO(hpo)_2]$ in CH_2Cl_2, one can confirm that the species present both at RT and at 120 K is the square pyramidal complex.

Concerning the octahedral complex formed by $[VO(hpo)_2]$ in DMSO, DFT calculations allow us to rule out the formation of the *trans*-octahedral isomers (Table 2).

Unfortunately, for both square pyramidal and *cis*-octahedral complexes, it is not possible to determine which of the possible isomers is formed because the hyperfine coupling constants are similar (see Table 2).

Analogous conclusions can be reached for the complex of mpo (see Supporting Information Table S3).

At this point one can conclude that in the equilibrium between the penta-coordinated and hexa-coordinated complex only the *cis*-octahedral species is involved (Scheme 2). With the ligands considered here, the preferred coordination geometry is square pyramidal in non-coordinating solvents, while is *cis*-octahedral in coordinating solvents (especially for hpo). This means that a coordinating solvent molecule leads to more stable complexes after its binding in equatorial position than in the axial one; the formation of *trans*-octahedral species is rarely observed in the literature.

The involvement of monochelated complexes, $[VO(hpo)(H_2O)_2]^+$ and/or $[VO(hpo)(H_2O)_3]^+$, in equilibria can be ruled out because much larger A_{iso} and A_z values should be obtained.

Calculation of the Influence of the Temperature on the Equilibrium

The equilibrium included in Scheme 2 (where S is modeled by H_2O) can be written as

$$[VOL_2] + H_2O \rightleftarrows \textit{cis}\text{-}[VOL_2(H_2O)] \quad (1)$$

This equilibrium can be shifted, as shown before, to the right by decreasing the temperature and to the left by increasing it.

To know which species are more stable at one specific temperature the variation of Gibbs energy (ΔG^{tot}) can be calculated, that is the difference between the Gibbs energy of the products and of the reactants:

$$\Delta G^{tot} = G^{tot}_{\textit{cis}\text{-}[VOL_2(H_2O)]} - (G^{tot}_{[VOL_2]} + G^{tot}_{H_2O}) \quad (2)$$

If ΔG^{tot} value is negative, the more stable species is *cis*-$[VOL_2(H_2O)]$, while if the value is positive, the more stable species is $[VOL_2]$. Comparing the value of ΔG^{tot} at two different temperatures (120 and 298.15 K), it is possible to determine the influence of the temperature.

The Gibbs energy can be computed using Gaussian software.

It is important to know that the Gibbs energy in solution for a given molecule at one specific temperature consists in a sum of different terms; the exact procedure to derive the value of ΔG^{tot} is reported in the Supporting Information and literature.[12,19]

The results obtained by DFT calculations for the complex of hpo allow us to conclude that the formation of $[VO(hpo)_2]$ is favored by high temperature (at 298.15 K, ΔG^{tot} = 11.3 kJ mol^{-1}), while at low temperature, the equilibrium is shifted toward the species *cis*-$[VO(hpo)_2(H_2O)]$ (at 120 K, ΔG^{tot} = −14.0 kJ mol^{-1}). The ΔG^{tot} values are obtained using for $G^{tot}_{\textit{cis}-[VO(hpo)_2(H_2O)]}$ the average of the values of the complexes *OC*-6-23, *OC*-6-24, *OC*-6-32 and *OC*-6-34, while for $G^{tot}_{[VO(hpo)_2]}$, the average of the values of the species *SPY*-5-12 and *SPY*-5-13 was used (see Supporting Information Table S6).

The same calculations could be performed also for mpo complexes.

■ ASSOCIATED CONTENT

Ⓢ Supporting Information

A detailed description of the experiment, including the background EPR spectroscopy and detailed students' instructions. This material is available via the Internet at http://pubs.acs.org.

■ AUTHOR INFORMATION

Corresponding Author

*Fax: (+39)-079-2841299. E-mail: Daniele.Sanna@ss.icb.cnr.it.

Notes

The authors declare no competing financial interest.

■ REFERENCES

(1) (a) Ophardt, C. E. Cobalt complexes in equilibrium. *J. Chem. Educ.* **1980**, *57* (6), 453−453. (b) Spears, L. G.; Spears, L. G. Chemical storage of solar energy using an old color change demonstration. *J. Chem. Educ.* **1984**, *61* (3), 252−254. (c) Grant, A. W. Cobalt complexes and Le Châtelier. *J. Chem. Educ.* **1984**, *61* (5), 466.

(2) Sanna, D.; Ugone, V.; Micera, G.; Garribba, E. Temperature and solvent structure dependence of VO^{2+} complexes of pyridine-N-oxide

DOI: 10.1021/ed500794m
J. Chem. Educ. XXXX, XXX, XXX−XXX

derivatives and their interaction with human serum transferrin. *Dalton Trans.* **2012**, *41* (24), 7304−7318.
(3) Equilibria involving bis-chelated oxidovanadium(IV) complexes are depicted in Scheme 2 while more details about the chemistry of this element can be found in Rehder, D.; *Bioinorganic Vanadium Chemistry*; John Wiley & Sons, Ltd: New York, 2008.
(4) Sakurai, H.; Tamura, A.; Fugono, J.; Yasui, H.; Kiss, T. New antidiabetic vanadyl−pyridone complexes: effect of equivalent transformation of coordinating atom in the ligand. *Coord. Chem. Rev.* **2003**, *245* (1−2), 31−37.
(5) Higes-Rolando, F. J.; Perez-Florindo, A.; Valenzuela-Calahorro, C.; Martin-Ramos, J. D.; Romero-Garzon, J. Oxobis(N-oxopyridine-2-thiolato-N,O)vanadium(IV). *Acta Crystallogr., Sect. C* **1994**, *50* (7), 1049−1052.
(6) Tsagkalidis, W.; Rodewald, D.; Rehder, D.; Vergopoulos, V. Bis(2-mercaptopyridine-N-oxide)oxovanadium(IV): Synthesis, structure and its conversion to the dichloro complex. *Inorg. Chim. Acta* **1994**, *219* (1−2), 213−215.
(7) (a) Basu, P. Use of EPR spectroscopy in elucidating electronic structures of paramagnetic transition metal complexes. *J. Chem. Educ.* **2001**, *78* (5), 666−669. (b) Bunce, N. J. Introduction to the interpretation of electron spin resonance spectra of organic radicals. *J. Chem. Educ.* **1987**, *64* (11), 907−914.
(8) (a) Butera, R. A.; Waldeck, D. H. An EPR experiment for the undergraduate physical chemistry laboratory. *J. Chem. Educ.* **2000**, *77* (11), 1489. (b) Garribba, E.; Micera, G. The determination of the geometry of Cu(II) complexes: An EPR spectroscopy experiment. *J. Chem. Educ.* **2006**, *83* (8), 1229−1232. (c) Linenberger, K.; Bretz, S. L.; Crowder, M. W.; McCarrick, R.; Lorigan, G. A.; Tierney, D. L. What Is the true color of fresh meat? A biophysical undergraduate laboratory experiment investigating the effects of ligand binding on myoglobin using optical, EPR, and NMR spectroscopy. *J. Chem. Educ.* **2010**, *88* (2), 223−225.
(9) Haddy, A. Using a molecular modeling program to calculate electron paramagnetic resonance hyperfine couplings in semiquinone anion radicals. *J. Chem. Educ.* **2001**, *78* (9), 1206.
(10) *WINEPR SimFonia*, version 1.25; Bruker Analytische Messtechnik GmbH: Karlshrue, 1996.
(11) Stoll, S.; Schweiger, A. EasySpin, a comprehensive software package for spectral simulation and analysis in EPR. *J. Magn. Reson.* **2006**, *178* (1), 42−55.
(12) (a) Lodyga-Chruscinska, E.; Micera, G.; Garribba, E. Complex formation in aqueous solution and in the solid state of the potent insulin-enhancing $V^{IV}O^{2+}$ compounds formed by picolinate and quinolinate derivatives. *Inorg. Chem.* **2011**, *50* (3), 883−899. (b) Sanna, D.; Buglyó, P.; Bíró, L.; Micera, G.; Garribba, E. Coordinating properties of pyrone and pyridinone derivatives, tropolone and catechol toward the VO^{2+} Ion: An experimental and computational approach. *Eur. J. Inorg. Chem.* **2012**, *7*, 1079−1092.
(13) Frozen solution is referred both to 77 K, that is the liquid nitrogen temperature, and to 120 K, the temperature at which EPR spectra were measured. Both these will be indicated as low temperature (LT).
(14) (a) Freitag, R.; Conradie, J. Understanding the Jahn−Teller effect in octahedral transition-metal complexes: A molecular orbital view of the Mn(β-diketonato)$_3$ complex. *J. Chem. Educ.* **2013**, *90* (12), 1692−1696. (b) Montgomery, C. D. π Backbonding in carbonyl complexes and carbon−oxygen stretching frequencies: A molecular modeling exercise. *J. Chem. Educ.* **2007**, *84* (1), 102−105. (c) Pernicone, N. C.; Geri, J. B.; York, J. T. Using a combination of experimental and computational methods to explore the impact of metal identity and ligand field strength on the electronic structure of metal ions. *J. Chem. Educ.* **2011**, *88* (9), 1323−1327.
(15) Frisch, M. J.; Trucks, G. W.; Schlegel, H. B.; Scuseria, G. E.; Robb, M. A.; Cheeseman, J. R.; Montgomery, J. A., Jr.; Vreven, T.; Kudin, K. N.; Burant, J. C.; Millam, J. M.; Iyengar, S. S.; Tomasi, J.; Barone, V.; Mennucci, B.; Cossi, M.; Scalmani, G.; Rega, N.; Petersson, G. A.; Nakatsuji, H.; Hada, M.; Ehara, M.; Toyota, K.; Fukuda, R.; Hasegawa, J.; Ishida, M.; Nakajima, T.; Honda, Y.; Kitao, O.; Nakai, H.; Klene, M.; Li, X.; Knox, J. E.; Hratchian, H. P.; Cross, J. B.; Adamo, C.; Jaramillo, J.; Gomperts, R.; Stratmann, R. E.; Yazyev, O.; Austin, A. J.; Cammi, R.; Pomelli, C.; Ochterski, J. W.; Ayala, P. Y.; Morokuma, K.; Voth, G. A.; Salvador, P.; Dannenberg, J. J.; Zakrzewski, V. G.; Dapprich, S.; Daniels, A. D.; Strain, M. C.; Farkas, O.; Malick, D. K.; Rabuck, A. D.; Raghavachari, K.; Foresman, J. B.; Ortiz, J. V.; Cui, Q.; Baboul, A. G.; Clifford, S.; Cioslowski, J.; Stefanov, B. B.; Liu, G.; Liashenko, A.; Piskorz, P.; Komaromi, I.; Martin, R. L.; Fox, D. J.; Keith, T.; Al-Laham, M. A.; Peng, C. Y.; Nanayakkara, A.; Challacombe, M.; Gill, P. M. W.; Johnson, B.; Chen, W.; Wong, M. W.; Gonzalez, C.; Pople, J. A. *Gaussian 03*, revision C.02; Gaussian, Inc.: Wallingford, CT, 2004.
(16) Micera, G.; Garribba, E. The effect of the functional, basis set, and solvent in the simulation of the geometry and spectroscopic properties of $V^{IV}O^{2+}$ complexes. Chemical and biological applications. *Int. J. Quantum Chem.* **2012**, *112* (12), 2486−2498.
(17) (a) Micera, G.; Garribba, E. On the prediction of ^{51}V hyperfine coupling constants in $V^{IV}O$ complexes through DFT methods. *Dalton Trans.* **2009**, *11*, 1914−1918. (b) Gorelsky, S.; Micera, G.; Garribba, E. The equilibrium between the octahedral and square pyramidal form and the influence of an axial ligand on the molecular properties of $V^{IV}O$ complexes: A spectroscopic and DFT study. *Chem.−Eur. J.* **2010**, *16* (27), 8167−8180. (c) Micera, G.; Garribba, E. Application of DFT methods in the study of $V^{IV}O^{2+}$-peptide interactions. *Eur. J. Inorg. Chem.* **2010**, *29*, 4697−4710. (d) Micera, G.; Garribba, E. Is the spin-orbit coupling important in the prediction of the ^{51}V hyperfine coupling constants of $V^{IV}O^{2+}$ species? ORCA versus Gaussian performance and biological applications. *J. Comput. Chem.* **2011**, *32* (13), 2822−2835. (e) Micera, G.; Garribba, E. The effect of trigonal bipyramidal distortion of pentacoordinate $V^{IV}O^{2+}$ species on their sructural, electronic and spectroscopic parameters. *Eur. J. Inorg. Chem.* **2011**, *25*, 3768−3780. (f) Sanna, D.; Biro, L.; Buglyo, P.; Micera, G.; Garribba, E. Transport of the anti-diabetic VO^{2+} complexes formed by pyrone derivatives in the blood serum. *J. Inorg. Biochem.* **2012**, *115*, 87−99.
(18) *Nomenclature of Inorganic Chemistry—IUPAC Recommendations*; Connelly, N. G., Damhus, T., Hartshorn, R. M., Hutton, A. T., Eds.; The Royal Society of Chemistry: Cambridge, 2005.
(19) (a) Sanna, D.; Varnágy, K.; Timári, S.; Micera, G.; Garribba, E. VO^{2+} complexation by bioligands showing keto-enol tautomerism: A potentiometric, spectroscopic, and computational study. *Inorg. Chem.* **2011**, *50* (20), 10328−10341. (b) Sanna, D.; Várnagy, K.; Lihi, N.; Micera, G.; Garribba, E. Formation of new non-oxido vanadium(IV) species in aqueous solution and in the solid state by tridentate (O, N, O) ligands and rationalization of their EPR behavior. *Inorg. Chem.* **2013**, *52*, 8202−8213.

DOI: 10.1021/ed500794m
J. Chem. Educ. XXXX, XXX, XXX−XXX